J|A|C|S
ARTICLES
Published on Web 02/02/2006

Self-Assembly of Block Copolymer Micelles in an Ionic Liquid

Yiyong He,[†] Zhibo Li,[†] Peter Simone,[†] and Timothy P. Lodge*[,†,‡]

Contribution from the Departments of Chemistry and Chemical Engineering and Materials Science, University of Minnesota, Minneapolis, Minnesota 55455

Received December 8, 2005; E-mail: lodge@chem.umn.edu

Abstract: Four amphiphilic poly((1,2-butadiene)-*block*-ethylene oxide) (PB−PEO) diblock copolymers were shown to aggregate strongly and form micelles in an ionic liquid, 1-butyl-3-methylimidazolium hexafluorophosphate ([BMIM][PF_6]). The universal micellar structures (spherical micelle, wormlike micelle, and bilayered vesicle) were all accessed by varying the length of the corona block while holding the core block constant. The nanostructures of the PB−PEO micelles formed in an ionic liquid were directly visualized by cryogenic transmission electron microscopy (cryo-TEM). Detailed micelle structural information was extracted from both cryo-TEM and dynamic light scattering measurements, with excellent agreement between the two techniques. Compared to aqueous solutions of the same copolymers, [BMIM][PF_6] solutions exhibit some distinct features, such as temperature-independent micellar morphologies between 25 and 100 °C. As in aqueous solutions, significant nonergodicity effects were also observed. This work demonstrates the flexibility of amphiphilic block copolymers for controlling nanostructure in an ionic liquid, with potential applications in many arenas.

Introduction

The self-assembly of amphiphilic molecules into discrete nanostructures is of fundamental interest and is important in many applications, including nanolithography,[1] nanomaterial synthesis,[2−4] drug delivery,[5,6] separation,[7] pharmaceutical formulation,[7] and other dispersant technologies.[7] Block copolymers offer potential advantages over conventional low molar mass surfactants and lipids in their remarkable design flexibility for controlling nanostructure and functionality, through molecular weight, composition, architecture, and choice of monomer units.[8−14] Diverse selectivity and functionality possessed by different types of solvents further enrich this self-assembly toolbox.[9,15,16]

Due to their many attractive properties, ionic liquids have received increasing attention recently. In comparison to common volatile organic solvents, ionic liquids are appealing for environmental reasons as well as for providing unprecedented solvation tunability. Negligibly small vapor pressure, fire resistance, excellent chemical and thermal stability, wide liquid temperature ranges, and wide electrochemical windows are examples of the useful properties typical of ionic liquids.[15,17] Ionic liquids have been considered for use in organic synthesis,[18,19] chemical separation,[20,21] hazardous chemical storage and transportation,[22] and polymer gel electrolytes,[23,24] and their applications continue to expand. However, even with a growing number of ionic liquids becoming commercially available, most ionic liquids are currently too expensive for industrial-scale applications. Toxicity and environmental compatibility studies of ionic liquids are rare, which does raise some concerns about their environmental benefits.

[†] Department of Chemistry.
[‡] Department of Chemical Engineering and Materials Science.

(1) Park, M.; Harrison, C.; Chaikin, P. M.; Register, R. A.; Adamson, D. H. *Science* **1997**, *276*, 1401−1404.
(2) Jaramillo, T. F.; Baeck, S. H.; Cuenya, B. R.; McFarland, E. W. *J. Am. Chem. Soc.* **2003**, *125*, 7148−7149.
(3) Sohn, B. H.; Choi, J. M.; Yoo, S. I.; Yun, S. H.; Zin, W. C.; Jung, J. C.; Kanehara, M.; Hirata, T.; Teranishi, T. *J. Am. Chem. Soc.* **2003**, *125*, 6368−6369.
(4) Massey, J. A.; Winnik, M. A.; Manners, I.; Chan, V. Z. H.; Ostermann, J. M.; Enchelmaier, R.; Spatz, J. P.; Moller, M. *J. Am. Chem. Soc.* **2001**, *123*, 3147−3148.
(5) Savic, R.; Luo, L. B.; Eisenberg, A.; Maysinger, D. *Science* **2003**, *300*, 615−618.
(6) Allen, C.; Maysinger, D.; Eisenberg, A. *Colloids Surf., B* **1999**, *16*, 3−27.
(7) Alexandridis, P., Lindman, B., Eds. *Amphiphilic Block Copolymers: Self-Assembly and Applications*; Elsevier: Amsterdam, 2000.
(8) Hawker, C. J.; Wooley, K. L. *Science* **2005**, *309*, 1200−1205.
(9) Lodge, T. P.; Bang, J. A.; Li, Z. B.; Hillmyer, M. A.; Talmon, Y. *Faraday Discuss.* **2005**, *128*, 1−12.
(10) Li, Z. B.; Kesselman, E.; Talmon, Y.; Hillmyer, M. A.; Lodge, T. P. *Science* **2004**, *306*, 98−101.
(11) Zhou, Z. L.; Li, Z. B.; Ren, Y.; Hillmyer, M. A.; Lodge, T. P. *J. Am. Chem. Soc.* **2003**, *125*, 10182−10183.
(12) Kotzev, A.; Laschewsky, A.; Adriaensens, P.; Gelan, J. *Macromolecules* **2002**, *35*, 1091−1101.
(13) Gohy, J. F.; Willet, N.; Varshney, S.; Zhang, J. X.; Jerome, R. *Angew. Chem., Int. Ed.* **2001**, *40*, 3214−3216.
(14) Liu, S. Y.; Armes, S. P. *J. Am. Chem. Soc.* **2001**, *123*, 9910−9911.
(15) Hoffmann, M. M.; Heitz, M. P.; Carr, J. B.; Tubbs, J. D. *J. Dispersion Sci. Technol.* **2003**, *24*, 155−171.
(16) Kesselman, E.; Talmon, Y.; Bang, J.; Abbas, S.; Li, Z. B.; Lodge, T. P. *Macromolecules* **2005**, *38*, 6779−6781.
(17) Huddleston, J. G.; Visser, A. E.; Reichert, W. M.; Willauer, H. D.; Broker, G. A.; Rogers, R. D. *Green Chem.* **2001**, *3*, 156−164.
(18) Zerth, H. M.; Leonard, N. M.; Mohan, R. S. *Org. Lett.* **2003**, *5*, 55−57.
(19) Yadav, J. S.; Reddy, B. V. S.; Gayathri, K. U.; Prasad, A. R. *Synthesis* **2002**, *17*, 2537−2541.
(20) Anderson, J. L.; Ding, J.; Welton, T.; Armstrong, D. W. *J. Am. Chem. Soc.* **2002**, *124*, 14247−14254.
(21) Anderson, J. L.; Armstrong, D. W. *Anal. Chem.* **2005**, *77*, 6453−6462.
(22) Freemantle, M. *Chem. Eng. News* **2005**, *83* (Aug 1), 33−38.
(23) Ohno, H.; Yoshizawa, M.; Ogihara, W. *Electrochim. Acta* **2003**, *48*, 2079−2083.
(24) Susan, M. A.; Kaneko, T.; Noda, A.; Watanabe, M. *J. Am. Chem. Soc.* **2005**, *127*, 4976−4983.

Surprisingly, perhaps, there has been relatively little attention paid to ionic liquids as solvation media for polymer systems.[15,25] Nor has the utility of polymers for structuring ionic liquids been extensively explored, e.g., as micelles, microemulsions, and gels.[24] Recently there have been some reports on the micellization of low molar mass surfactants in ionic liquids.[26−29] It is the purpose of this work to report the first study of block copolymer micellization in an ionic liquid, and further to demonstrate direct visualization of the various self-assembled nanostructures by cryogenic transmission electron microscopy (cryo-TEM). The self-assembly of diblock copolymers in selective solvents to form micelles is well documented. The predominant micellar morphologies are spheres, with cylindrical micelles ("worms") and bilayered vesicles (the shell of the vesicle comprising bilayered copolymer sheets) also reported.[30−32] The morphology is determined by the free energy balance among the chain stretching in the core, the core−corona interfacial energy, and the repulsion between coronal chains.[33,34] In practice, the micellar morphology can be manipulated through the choice of monomers, block copolymer composition and molecular weight, solvent selectivity, and external stimuli such as temperature, pH, and ionic strength.[9]

This work investigates the micellization of four poly((1,2-butadiene)-*block*-ethylene oxide) diblock copolymers (PB−PEO) in 1-butyl-3-methylimidazolium hexafluorophosphate ([BMIM][PF_6]), where [BMIM][PF_6] is a good solvent for PEO. Several factors have guided the selection of this system. [BMIM][PF_6] is the most commonly used ionic liquid at room temperature and is less moisture sensitive than many other imidazolium analogues. PB has a glass transition temperature (~ -12 °C)[35] that is well below room temperature and thus avoids the complicated equilibration issue in the case of glassy core domains. The electron density difference between PB and [BMIM][PF_6] is substantial, which facilitates "natural-contrast" imaging of micellar nanostructures by cryo-TEM.

We demonstrate that amphiphilic block copolymers are able to form well-defined micelles in [BMIM][PF_6]. All three "universal" micellar morphologies—spherical micelles, wormlike micelles, and bilayered vesicles—were observed upon varying the length of the PEO block. The micelles were directly visualized by cryo-TEM; as far as we are aware, this represents the first demonstration of this powerful technique in an ionic liquid. With the aid of dynamic light scattering (DLS), the detailed packing characteristics of the micelles were extracted and compared to the results for the same copolymers in water.[36] The molecular characteristics of the PB−PEO diblock copolymers are listed in Table 1; more detailed sample and experimental information (including equations) can be obtained from the Supporting Information.

Table 1. Molecular Characterization of PB−PEO Diblock Copolymers[a]

sample code	M_{PB} (kg/mol)	M_{PEO} (kg/mol)	PDI[b]	f_{PEO}[c]
BO(9−20)	9.2	21.0	1.09	0.64
BO(9−10)	9.2	9.9	1.06	0.45
BO(9−7)	9.2	7.2	1.05	0.38
BO(9−4)	9.2	4.0	1.06	0.25

[a] Information was reproduced from ref 37. PB block microstructures reflect 90% 1,2-addition. [b] Polydispersity index, by size exclusion chromatography. [c] Volume fraction of PEO block, by ^{1}H NMR.

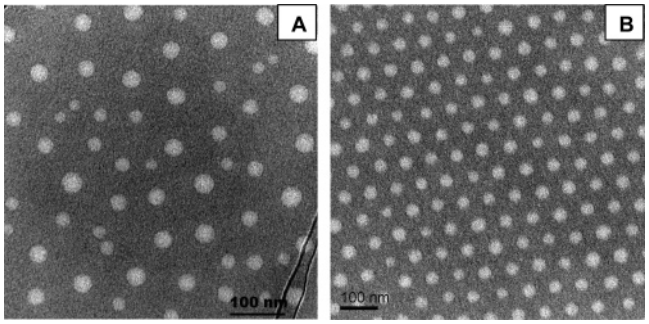

Figure 1. Cryo-TEM images of 1 wt % [BMIM][PF_6] solutions: (A) BO(9−20) ($f_{PEO} = 0.64$); (B) BO(9−10) ($f_{PEO} = 0.45$). Bright PB micellar cores were visualized.

Results and Discussion

Cryo-TEM Imaging of PB−PEO Micelles. The self-assembled morphology of the four PB−PEO diblock copolymers in [BMIM][PF_6] was examined with cryo-TEM. Figure 1A provides a representative image for BO(9−20), which clearly shows spherical micelles formed in a 1 wt % [BMIM][PF_6] solution. The bright spheres correspond to the PB micellar cores (lower electron density region) embedded in the [BMIM][PF_6] matrix (higher electron density region). The mean core radius (averaging over more than 200 spheres) is 15.2 nm. The PEO corona chains are not directly visible as they are well solvated, but their presence and dimensions are reflected by the typical separation between neighboring cores. In Figure 1A, the mean micelle separation is estimated to be 88 nm by simply calculating the two-dimensional density of objects. A further notable feature of Figure 1A is that the image contrast is reversed with respect to cryo-TEM images in an aqueous medium;[36,37] the same effect was recently reported for poly(styrene-*block*-isoprene) diblock copolymer micelles in dialkyl phthalates.[16,38]

BO(9−10) forms spherical micelles similar to those formed by BO(9−20), as shown in Figure 1B. The micelle size distribution is apparently narrower for BO(9−10) than for BO(9−20), but this is most likely an artifact of the limited field of view; the DLS measurements to be presented indicate a similarly narrow distribution. A significant feature of Figure 1B is the regular hexagonal packing of the spheres, with a mean separation of about 76 nm. The regularity in micelle packing is induced by the sample preparation process; the solution itself,

(25) Brazel, C. S., Rogers, R. D., Eds. *Ionic Liquids in Polymer Systems: Solvents, Additives, and Novel Applications*; American Chemical Society: Washington, DC, 2005 (distributed by Oxford University Press).
(26) Eastoe, J.; Gold, S.; Rogers, S. E.; Paul, A.; Welton, T.; Heenan, R. K.; Grillo, I. *J. Am. Chem. Soc.* **2005**, *127*, 7302−7303.
(27) Atkin, R.; Warr, G. G. *J. Am. Chem. Soc.* **2005**, *127*, 11940−11941.
(28) Araos, M. U.; Warr, G. G. *J. Phys. Chem. B* **2005**, *109*, 14275−14277.
(29) Anderson, J. L.; Pino, V.; Hagberg, E. C.; Sheares, V. V.; Armstrong, D. W. *Chem. Commun.* **2003**, 2444−2445.
(30) Zhang, L. F.; Eisenberg, A. *Science* **1995**, *268*, 1728−1731.
(31) Won, Y. Y.; Davis, H. T.; Bates, F. S. *Science* **1999**, *283*, 960−963.
(32) Discher, B. M.; Won, Y. Y.; Ege, D. S.; Lee, J. C. M.; Bates, F. S.; Discher, D. E.; Hammer, D. A. *Science* **1999**, *284*, 1143−1146.
(33) Halperin, A.; Tirrell, M.; Lodge, T. P. *Adv. Polym. Sci.* **1992**, *100*, 31−71.
(34) Hamley, I. W. *The physics of block copolymers*; Oxford University Press: Oxford, New York, 1998.
(35) He, Y. Y.; Lutz, T. R.; Ediger, M. D. *Macromolecules* **2004**, *37*, 9889−9898.
(36) Jain, S.; Bates, F. S. *Science* **2003**, *300*, 460−464.
(37) Jain, S.; Bates, F. S. *Macromolecules* **2004**, *37*, 1511−1523.
(38) Bang, J.; Jain, S.; Li, Z. B.; Lodge, T. P.; Pedersen, J. S.; Kesselman, E.; Talmon, Y. *Macromolecules*, published online Jan 4, http://dx.doi.org/10.1021/ma052023+.

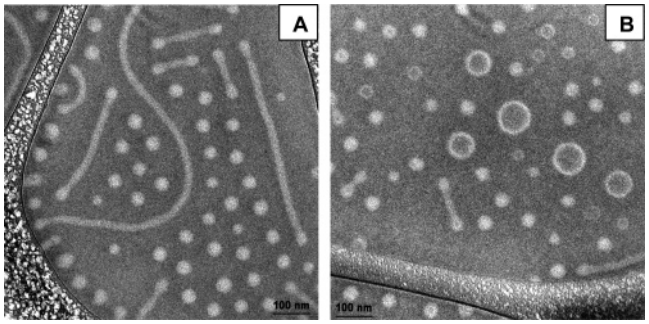

Figure 2. Cryo-TEM images of 1 wt % BO(9−7) (f_{PEO} = 0.38) in [BMIM][PF_6]. There is a coexistence of spherical and wormlike micelles (panel A), along with some vesicles (panel B).

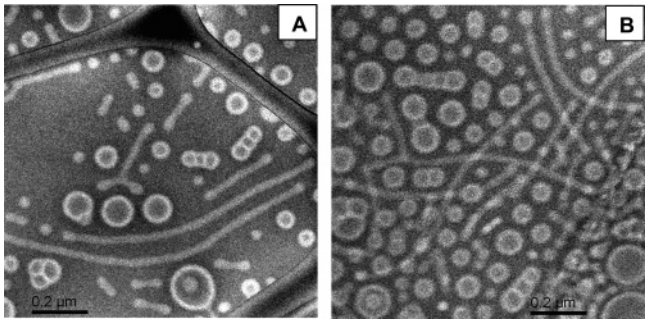

Figure 3. Cryo-TEM images of 1 wt % BO(9−4) (f_{PEO} = 0.25) in [BMIM][PF_6]. There is a coexistence of wormlike micelles and vesicles.

of course, is a dilute suspension of independent micelles. The regular packing in Figure 1B, compared to Figure 1A, is attributable to the more hard-sphere-like interaction of the micelles with shorter corona chains. Compared to BO(9−20), BO(9−10) has a shorter PEO block and forms micelles with denser coronas, as will be quantified subsequently. There is some overlap of micelle coronas in Figure 1A which is absent in Figure 1B.

Further decreasing the PEO block length leads to the formation of wormlike micelles and bilayered vesicles. This is illustrated in Figure 2A,B for BO(9−7), where there is a coexistence of spherical and wormlike micelles, along with some vesicles. Most of the wormlike micelles are less than 1 μm in length. Two spherical end caps with larger diameter are clearly resolved for each wormlike micelle. BO(9−4) has the smallest PEO block length of the four PB−PEO copolymers. Its self-assembled structure is dominated by wormlike micelles and bilayered vesicles (Figure 3). Figure 3 also discloses diverse vesicle morphologies, including some vesicle clusters and encapsulated vesicles. The wormlike micelles contain occasional Y-junctions (Figure 3A), which can be distinguished from micellar overlap (Figure 3B) by measuring the optical density at the crossing points; i.e., overlaps appear lighter than other parts of the micelles, whereas the optical density is uniform through Y-junctions. The coexistence of different morphologies in Figures 2 and 3 will be discussed in a later section.

As a brief summary, by varying the PEO composition f_{PEO} from 0.64 to 0.25, the "universal" sequences of diblock copolymer micellar structures (spheres, wormlike micelles, and bilayered vesicles) were all resolved in 1 wt % [BMIM][PF_6] solutions. Decreasing f_{PEO} causes transitions from spheres to wormlike micelles to bilayered vesicles, in the order of decreasing core−corona interfacial curvature. Qualitatively, the structural change with the variation of copolymer composition resembles those previously documented in water[36,39] and organic solvents.[40] As the PB block length is fixed for the four PB−PEO copolymers, the interfacial curvature increases with increasing f_{PEO} to accommodate the relatively longer solvent-compatible PEO blocks in the corona domain. The micellar structures revealed by cryo-TEM are also consistent with the results obtained from visual observation and light scattering. Visual observation provides a qualitative hint about the morphologies and dimensions of the colloidal domains, as the solution turbidity reflects the presence of particles with sizes comparable to the wavelength of light. The 1 wt % solutions of BO(9−20) (spheres), BO(9−10) (spheres), BO(9−7) (spheres and wormlike micelles), and BO(9−4) (wormlike micelles and vesicles) appear bluish clear, bluish clear, slight cloudy, and cloudy, respectively. The DLS results will be presented and compared to cryo-TEM results later, but the agreement is very satisfactory.

Table 2. Packing Characteristics of PB−PEO Block Copolymer Micelles Formed in 1 wt % [BMIM][PF_6] Solutions

sample code	R_c[a] (nm)	a_0 (nm^2)	s[b]	p	R_h[c] (nm)	μ_2/Γ^2	$R_h - R_c$ (nm)	$\langle h_0^2\rangle_{PEO}^{1/2}$[b] (nm)
BO(9−20)	15.2 (S)	3.4	2.0	840	46	0.08	30.8	14.7
BO(9−10)	18.6 (S)	2.8	2.4	1540	36	0.07	17.4	10.1
BO(9−7)	20.7 (S)	2.5	2.7	2120	54	0.36		8.6
	12.0 (C)	2.9[d]	1.5	26[d]				
BO(9−4)	14.5 (C)	2.4[d]	1.9	38[d]	97	0.39		6.4
	12.0 (B)	1.5[e]	1.5	1.5[e]				

[a] Core domain sizes: radius for spheres (S) and wormlike micelle (C), and half-thickness for bilayered vesicle (B). The uncertainty is ±2 nm. [b] The root-mean-square end-to-end distance of unperturbed PB chains is 7.8 nm. The unperturbed chain dimensions of PB and PEO were estimated using characteristic ratios of C_∞(PB) = 7.6 and C_∞(PEO) = 6.7 (see ref 41). [c] Apparent hydrodynamic radii with ±5% uncertainty. [d] p corresponds to a unit length (1 nm) of each wormlike micelle, calculated from its volume and the known PB bulk density (ρ_{PB} = 0.87 g/cm^3, see ref 42). [e] p corresponds to a unit area (1 nm^2) of each bilayered vesicle, calculated from its volume and the PB bulk density.

Packing Characteristics of Micelles. The high resolution of the cryo-TEM images leads to direct determination of the micelle core domain size. The radius of spheres (S) and wormlike micelles (C) and the half-thickness of bilayered vesicles (B) were measured by tracing the optical density profile as a function of distance across the respective core domains. The results are listed in Table 2 as R_c. For the spherical micelles formed by BO(9−20), BO(9−10), and BO(9−7), R_c increases from 15.2 to 18.6 to 20.7 nm, in the order of decreasing interfacial curvature. Since the three PB−PEO samples have constant PB block length, a scaling relationship could be established between R_c and the PEO block length (N_{PEO}) for spherical micelles: $R_c \propto N_{PEO}^{-0.28}$. This is a slightly stronger dependence on coronal chain length than most models predict;[34] in those models the predicted power law exponents fall in the range of −0.17 to −0.01. From a free energy standpoint this relationship between R_c and N_{PEO} is qualitatively understandable, since a shorter PEO block length reduces the corona crowding and permits a larger aggregation number. Further expansion of

(39) Won, Y. Y.; Brannan, A. K.; Davis, H. T.; Bates, F. S. *J. Phys. Chem.* **2002**, *106*, 3354−3364.
(40) Ding, J. F.; Liu, G. J.; Yang, M. L. *Polymer* **1997**, *38*, 5497−5501.
(41) Rubinstein, M.; Colby, R. H. *Polymer Physics*; Oxford University Press: Oxford, New York, 2003.
(42) Fetters, L. J.; Lohse, D. J.; Richter, D.; Witten, T. A.; Zirkel, A. *Macromolecules* **1994**, *27*, 4639−4647.

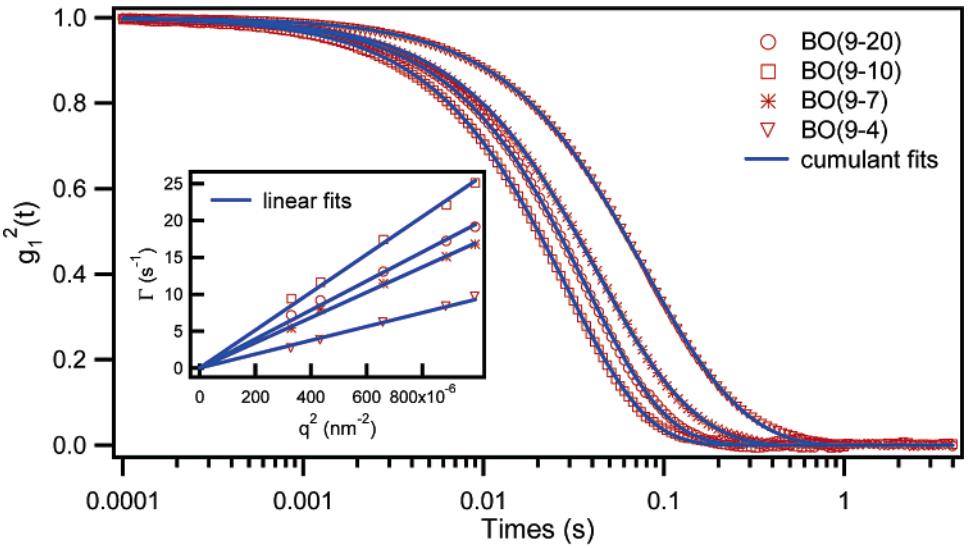

Figure 4. Normalized squared $g_1(q,t)$ correlation functions (measured by DLS at $\theta = 90°$ and 25.2 °C) of the four PB−PEO copolymers in 1 wt % [BMIM][PF_6] solutions. The solid lines are second moment cumulant fits. The inset shows linear fits of decay rate Γ vs q^2.

the spheres is inhibited by the large entropy penalty from stretching the PB chains in the core domains. Consequently, the micelles would rather adopt cylinder or vesicle forms to satisfy the interfacial curvature requirement when the PEO block is too short, as is the case for BO(9−7) and BO(9−4).

Quantitative characterization of the diverse micellar structures and packing properties can be achieved by calculating the interfacial area per chain (a_0), the chain stretching factor (s) for the PB block, and the aggregation number (p). Under the assumptions that the core domain is free of other components (i.e., [BMIM][PF_6] and PEO) and that there is a sharp interface between core and corona, the stretching factor s ($\equiv R_c/\langle h_0^2\rangle_{PB}^{1/2}$) can be taken as the ratio of the effective PB chain dimension to its unperturbed end-to-end length. Similarly, the aggregation number p can be calculated from the volume of the core domain and the PB bulk density, and the interfacial area per chain a_0 is the ratio of the core surface area to the aggregation number p. The values of a_0, s, and p are summarized in Table 2.

The correlation between the packing parameters and the micellar morphology (or copolymer composition) is delineated in Table 2. The constant PB block length simplifies the relationship. a_0 decreases almost monotonically with decreasing f_{PEO}; namely, the interfacial curvature becomes smaller when the solvent-compatible PEO chain becomes shorter. At an intermediate f_{PEO}, the PB chain stretching factor s reaches a maximum (the strongest aggregation), and that composition corresponds to the transition from spherical to wormlike micelles. In terms of different morphologies, the general trend is s(vesicle) < s(worm) < s(sphere). Values of the aggregation number p for the spheres are very large, indicating that the interfacial tension γ of PB−PEO is very large in [BMIM][PF_6]. These results may be contrasted to the pioneering work by Armstrong and co-workers.[29] They studied micelle formation for low molar mass surfactants (Brij700, Brij35, and caprylyl sulfobetaine) in [BMIM][PF_6] and found that the critical micelle concentration (CMC) is around 10 wt %, which indicates a very weak driving force for aggregation and a correspondingly small surface tension.

DLS Characterization. DLS is complementary to cryo-TEM, in that cryo-TEM enables direct visualization and determination of the nanostructures of individual micelles, while DLS measures the ensemble behavior of bulk solutions and thus provides important information such as the average hydrodynamic radius and its distribution.

Normalized squared electric field correlation functions $g_1(q,t)$ for the four PB−PEO copolymer solutions are shown in Figure 4. These measurements were taken at a scattering angle of 90° and room temperature. The second-order cumulant expansion (see eq 4 in the Supporting Information) fit the decay curves well, except possibly for a slight mismatch at long times. This observation suggests a monomodal distribution of micelle sizes. For each sample, the decay rate Γ measured at five different scattering angles displays excellent linearity versus q^2, as shown in the inset. The mutual diffusion coefficient D was extracted from the slope of Γ vs q^2 (eq 2), and the hydrodynamic radius R_h of the micelles can then be calculated from eq 3. The reduced second cumulant μ_2/Γ^2 is a measure of the width of the decay rate distribution G(Γ), and hence it gives an indication of dispersity of the micelle size. Both R_h and μ_2/Γ^2 are summarized in Table 2.

A significant feature of the micellization of PB−PEO in [BMIM][PF_6] is that the micelle size is temperature independent. For each sample, DLS experiments were performed at five different temperatures between 25 and 100 °C, and the variation of R_h and μ_2/Γ^2 was within experimental uncertainty. This result suggests that the good solvent character for PEO, or the nonsolvent character for PB, does not change significantly over this temperature range. Further exploration of the temperature dependence at higher temperatures was inhibited by PEO degradation.

There is excellent consistency between the cryo-TEM and DLS results. In particular, there is quantitative agreement for the spherical micelles in Table 2. As revealed by cryo-TEM in Figure 1, the spheres are closely packed or nearly closely packed. The mean micelle separation distances are 88 and 76 nm for BO(9−20) and BO(9−10), respectively. This implies that the overall micelle radii are 44 and 38 nm, which are very close to the hydrodynamic radii R_h (46 and 36 nm) measured by DLS. The analogous comparison for BO(9−7) and BO(9−4) is impeded by the coexistence of multiple morphologies and

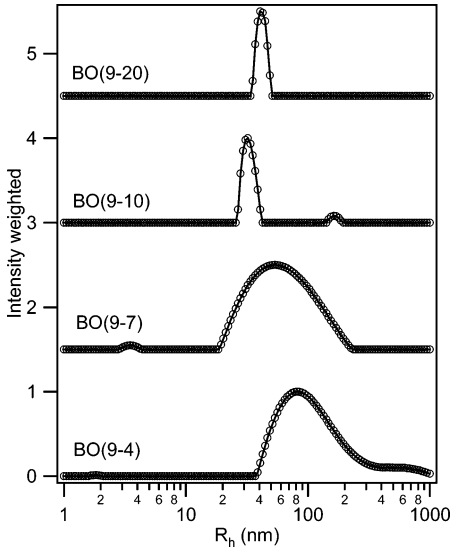

Figure 5. Apparent hydrodynamic radius distribution for the four PB−PEO copolymer micelles in 1 wt % [BMIM][PF_6] solutions, measured by DLS.

broader size distribution. However, DLS still provides a good estimate for the typical micelle dimensions, which are consistent with the cryo-TEM images. The narrow distribution of spherical micelles (Figure 1) and broad distribution of wormlike micelles and vesicles (Figures 2 and 3) are also reflected in the values of μ_2/Γ^2.

For the spherical micelles formed by BO(9−20) and BO(9−10), the structure of the corona can be inferred from the combined results of cryo-TEM and DLS. ($R_h - R_c$) is a good approximation for the corona thickness (Table 2). With the knowledge of the unperturbed end-to-end length for the PEO block, we can obtain the stretching factor for the corona. The values are 2.1 and 1.7 for BO(9−20) and BO(9−10), respectively. Correspondingly, the average volume fractions of PEO blocks in the corona domains are about 7% and 28%, calculated from the aggregation number p and approximate corona thickness ($R_h - R_c$). This supports the previous hypothesis that BO(9−10) micelles behave more like hard spheres than PB(9−20) micelles.

Micelle Size Distribution. In the cumulant analysis, the polydispersity of micelle dimension is indicated in the reduced second cumulant μ_2/Γ^2. An alternative way of extracting the micelle size distribution is to apply the inverse Laplace transformation directly to the measured correlation function.[43] The resulting decay rate distribution $G(\Gamma)$ was then transformed to hydrodynamic radius distribution through eqs 2−3 and presented in Figure 5.[44] The very narrow distributions of BO(9−20) and BO(9−10) micelles and broad distribution of BO(9−7) and BO(9−4) micelles are clearly shown in Figure 5. The results in Figure 5 agree well with cryo-TEM images. The tail at the larger R_h end for BO(9−4) is possibly due to some very long wormlike micelles and/or clusters of vesicles (hundreds of vesicles aggregating together, not shown in this paper).

Comparison to PB−PEO Self-Assembly in Water. Previous workers have investigated the micellar polymorphism of PB−PEO diblock copolymers in water[31,36,39,45] and the kinetic properties associated with the self-assembly process.[37,46] A comparison between the micellar nanostructures formed by PB−PEO in water and [BMIM][PF_6] provides a better understanding of the solvent properties and exposes some distinct features of [BMIM][PF_6]. Using the same samples as in a previous report[36] eliminates any ambiguity introduced by, e.g., molecular weight and chemical structural differences.

Table 3. Comparison of the Packing Parameters for 1 wt % PB−PEO in Water (H_2O) and Ionic Liquid (IL)

		R_c (nm)		a_0 (nm^2)		s	
copolymer	morphology	H_2O	IL	H_2O	IL	H_2O	IL
BO(9−20)	sphere	22.2	15.2	2.4	3.4	2.8	2.0
BO(9−4)	worm	15.8	14.5	2.2	2.4	2.0	1.9
	vesicle	8.8	12.0	2.0	1.5	1.1	1.5

The same sequence of micellar morphologies (sphere, wormlike micelle, and vesicle) and the trend with copolymer composition (f_{PEO}) were observed in both solvents. Both water and [BMIM][PF_6] are good solvents for the PEO block and nonsolvents for the PB block, so there is strong segregation of the core domains. A detailed comparison of the core domain dimension R_c, the interfacial area per chain a_0, and the stretching factor s for PB chains is summarized in Table 3. Although both systems are strongly segregated, the variation of packing parameters with f_{PEO} (or micellar morphology) is different. For the spheres formed by BO(9−20), and the worms formed by BO(9−4), the parameters in Table 3 indicated that water is the more selective solvent. On the other hand, for the vesicles formed by BO(9−4), the situation appears to be reversed. One possible interpretation is that, in the ionic liquid, the PB blocks are not interdigitated in the bilayer.[47] This leads to more stretching and a lower interfacial area per chain than in water. Other differences for PB−PEO self-assembly in [BMIM][PF_6] versus in water include the following: the sphere-to-worm boundary shifts toward lower f_{PEO} values,[36] the wormlike micelles are typically shorter,[31] and the micelle solutions seems to be more stable when exposed to a same electron dose.

One of the distinct features of PB−PEO micellization in [BMIM][PF_6] is the temperature independence of the micellar morphology over the temperature window 25−100 °C. The stable self-assembled nanostructures, combining the nonvolatile character of ionic liquids, offer great opportunities in nanomaterial synthesis and other dispersant technologies well above room temperature. As far as we are aware, there has been no report on the temperature dependence of PB−PEO micellization in water. However, significant temperature dependence has been observed in other PEO block copolymers, such as PEO−poly(propylene oxide) and PEO−poly(butylene oxide),[34] and attributed to the solvent character change for either or both components. The results here confirm, therefore, that [BMIM][PF_6] remains a very good solvent for PEO, and a very bad solvent for PB, over a wide temperature range.

It is also interesting to compare the affinity of PEO chains for water and [BMIM][PF_6]. Their relative affinity reverses with increasing temperature. A simple experiment has been done to demonstrate this phenomenon. An equal volume of water was added to a 1% BO(9−4) micelle solution in [BMIM][PF_6]. Since

(43) Provencher, S. W. *Comput. Phys. Commun.* **1982**, *27*, 213.
(44) Equation 3 is the Stokes-Einstein relation.
(45) Zheng, Y.; Won, Y. Y.; Bates, F. S.; Davis, H. T.; Scriven, L. E.; Talmon, Y. *J. Phys. Chem. B* **1999**, *103*, 10331−10334.
(46) Won, Y. Y.; Davis, H. T.; Bates, F. S. *Macromolecules* **2003**, *36*, 953−955.
(47) Battaglia, G.; Ryan, A. J. *J. Am. Chem. Soc.* **2005**, *127*, 8757−8764.

water and [BMIM][PF_6] are incompatible, two layers were observed, with water being the upper layer. After being stirred at room temperature for a few minutes, the lower layer changed from cloudy to clear, while the upper layer became cloudy. This indicates that PEO chains have stronger affinity to water than to [BMIM][PF_6] at room temperature, which is partly due to the formation of hydrogen bonds in water and is consistent with a recent study which showed that water is more polar than [BMIM][PF_6].[48] At temperatures above ~80 °C and following gentle stirring, the micelles then moved back from water to [BMIM][PF_6], and the lower layer became cloudy again. This is consistent with the known LCST behavior of PEO in water.[49,50]

Nonergodicity Effect on Micellar Morphology. A notable feature of Figures 2 and 3 is the coexistence of different micellar morphologies. Similar phenomena have been reported for the same block copolymers in water.[36,39] Considering the comparable PDI values (<1.1) for the four copolymers and nearly monodisperse micelles for BO(9−10) (Figure 1B), it is highly unlikely that molecular weight polydispersity is the dominant reason. Previous works have explored the molecular exchange kinetics in micelle solutions and its effect on micellar morphology.[37,46,51] For PB−PEO in water, it is found that there is no perceptible exchange of molecules between individual micellar objects over a time scale of several months.[37] In other words, the critical micelle concentration is vanishingly small, which is also true for PB−PEO in [BMIM][PF_6]. Therefore, the overall system is in a nonergodic state, and the initial micelle structures formed upon dissolution are more-or-less locked in. This nonergodicity effect is expected for block copolymers with strong amphiphilicity and relatively low solvent-compatible content.

Further observations support this explanation. For all four samples, DLS measurements performed one month after sample preparation show no difference from the measurements made immediately after sample preparation. More evidence comes from comparing cryo-TEM images of micelle solutions prepared from the same copolymer but by different routes. Both Figures 3 and 6 show representative cryo-TEM images of 1 wt % BO(9−4) in [BMIM][PF_6]. The solution in Figure 3 was made by direct mixing and stirring. The solution in Figure 6 was made by dissolving BO(9−4) and [BMIM][PF_6] in a cosolvent (CH_2Cl_2), followed by cosolvent evaporation. Both solutions were annealed at 70 °C for 1 day. Clearly, the wormlike micelles in Figure 3 are almost absent in Figure 6, suggesting that the wormlike micelle is a nonequilibrium morphology for BO(9−4) due to the nonergodicity effect. We speculate that the coexistence of multiple micellar morphologies in other samples is due to the same reason. The result shown here also suggests that one possible way to make equilibrium micelle solutions is to dissolve the solute and solvent in a cosolvent and then evaporate the cosolvent very slowly under stirring condition. This way is particularly suitable for ionic liquid solutions since ionic liquids are nearly nonvolatile.

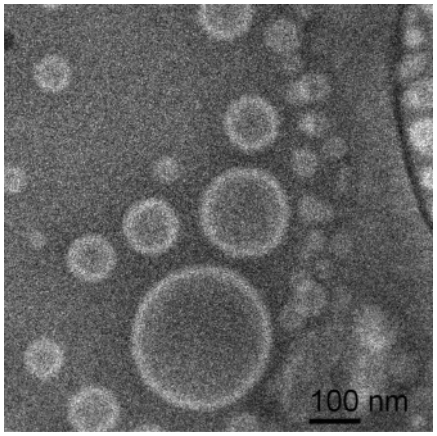

Figure 6. Cryo-TEM image of 1 wt % BO(9−4) in [BMIM][PF_6]. The solution was prepared using CH_2Cl_2 as cosolvent and followed by cosolvent evaporation. The morphology is different than that in Figure 3, the solution of which was made by direct mixing and stirring.

Conclusions

We have investigated the self-assembly of four PB−PEO diblock copolymers in an ionic liquid, [BMIM][PF_6]. It was shown that amphiphilic block copolymers are able to form well-defined micelles in ionic liquids, as in water and organic solvents. The micellar structures, in the universal sequence of spherical micelle, wormlike micelle, and bilayered vesicle, were all accessed by varying the PEO block length and directly visualized by cryo-TEM imaging. As far as we are aware, this represents the first demonstration of this powerful technique in an ionic liquid.

Detailed micelle structure information was extracted from the combined results of cryo-TEM and DLS, including the dimensions of the core and corona domains, the mean hydrodynamic radius and distribution, the aggregation number, and the chain stretching factor. There is excellent agreement between the micelle size and distribution measured by cryo-TEM and DLS.

Similar to their self-assembly in water, PB−PEO copolymers were strongly aggregated in [BMIM][PF_6], with aggregation numbers up to 2000 for spherical micelles. The nonergodicity effect on the micellar morphology was also observed. Besides the similarity, the aggregation of PB−PEO in [BMIM][PF_6] displays some distinct features, such as temperature independence of micellar morphologies between 25 and 100 °C.

This work demonstrates the feasibility of controlling micellar nanostructures of amphiphilic block copolymers in ionic liquids. The technique of cryo-TEM is shown to be very well-suited to direct imaging of such structures. In the effort to expand potential applications for ionic liquids, the results presented here provide a first step toward designing polymers to impart nanoscale structure in ionic liquid media, such as micelles, microemulsions, and ion gels.

Acknowledgment. This work was supported by the National Science Foundation through Award DMR-0406656. We thank Dr. Sumeet Jain for generously providing the block copolymers.

Supporting Information Available: Experimental details. This material is available free of charge via the Internet at http://pubs.acs.org.

JA058091T

(48) Reichardt, C. *Green Chem.* **2005**, *7*, 339−351.
(49) Dormidontova, E. E. *Macromolecules* **2004**, *37*, 7747−7761.
(50) Smith, G. D.; Bedrov, D. *J. Phys. Chem. B* **2003**, *107*, 3095−3097.
(51) Chen, L.; Shen, H. W.; Eisenberg, A. *J. Phys. Chem. B* **1999**, *103*, 9488−9497.